A Study of the Separation Principle in Size Exclusion Chromatography

Thomas Sun*

Baytown Polymers Center, ExxonMobil Chemical Company, 5200 Bayway Dr., Baytown, Texas 77520-2101

Ronald R. Chance, William W. Graessley,† and David J. Lohse

Corporate Strategic Research, ExxonMobil Research and Engineering, Annandale, New Jersey 08801

Received December 17, 2003; Revised Manuscript Received February 17, 2004

ABSTRACT: Size exclusion chromatography (SEC) separates polymer molecules according to their size in dilute solution, but what size to use has been a matter of debate for 35 years. In 1967, Benoit and co-workers found an excellent correlation between elution volume and a dynamically based molecular size, the hydrodynamic volume V_H, for a wide range of species and large-scale molecular architectures. However, both theory and simulations assume a thermodynamic separation principle. This assumption is based on experimental observations that elution volumes are independent of flow rates. Thus, one might surmise that the radius of gyration R_g is a more appropriate size measure for purposes of universal SEC calibration, although the calculations of Casassa and co-workers on star polymers suggest some other thermodynamically based size may be required. In an attempt to resolve this dilemma, we undertook an extensive study of SEC with three groups of nearly monodisperse polymers—linear polystyrenes, linear polyethylenes, and polyethylenes with several types of long chain branching. Measurements of R_g, molecular weight M, intrinsic viscosity $[\eta]$ ($V_H = [\eta]M$), and the elution volume on these various samples demonstrate that R_g correlates the partitioning of linear chains more satisfactorily than does V_H, while the reverse is true for branched chains. Extending the theoretical calculations of distribution coefficients for star polymers to other types of branched architectures may be necessary to settle the matter.

I. Introduction

Many polymeric properties depend on large-scale molecular architecture. The melt rheology of polymers, for example, cannot be understood without information about molecular weight distribution (MWD) and the distribution and types of long chain branching (LCB).[1−4] Size exclusion chromatography (SEC), introduced in 1964,[5] has evolved into the most widely used technique for providing such information.[6−8] However, despite the wide usage of SEC, an ambiguity about its separation principle has remained unresolved. Grubisic, Rempp, and Benoit in 1967 found that polymer molecules, regardless of species and differences in large-scale architecture,[9] separate according to a hydrodynamic volume $V_H \propto [\eta]M$, where $[\eta]$ is the intrinsic viscosity and M the molecular weight.[10] The authors did in fact consider the possibility of separation according to a geometrical size, the radius of gyration R_g. Although values of R_g were not available for their samples, they were nonetheless able to rule out that notion indirectly, from the good correlation already found with $[\eta]M$ and the known variations of $[\eta]$ and R_g with LCB architecture from other studies. The observed correlation based on $[\eta]M$ became accepted as the basis of universal GPC calibration.[6−8]

Still, the use of $[\eta]M$, a size based on dynamical properties, in the interpretation of SEC data is unsettling. Like other types of chromatography, SEC is typically run under low flow rate conditions where hydrodynamic factors should have little effect on the molecular partitioning.[6−8] Indeed, most theoretical descriptions of polymer molecules in pores use R_g as the size parameter.[11−16] To date, this issue has not been fully resolved. From theoretical considerations, Casassa and Tagami in 1969 concluded that R_g alone could not be the determining size parameter for symmetric stars, but they showed that thermodynamic considerations alone might still suffice.[12] In 1979, Roovers found that polystyrene linear and model comb polymers obey $[\eta]M$-based universal calibration but did not discuss the issue of R_g.[17] Similarly in 2002, Stogiou et al. showed that μ-stars, H-shaped, π-shaped, and linear tetrablock copolymers obey $[\eta]M$-based universal calibration, but they also did not discuss R_g.[18] On the other hand, Chance et al. showed in 1995 that the $[\eta]M$ correlation fails for low molecular weight linear polymers of different species.[19] Those results combined with molecular dynamics simulations suggested that R_g, although a better predictor of elution volume for linear chains than $[\eta]M$, is still insufficient.[19,20]

Here, we seek to address these separation mechanism uncertainties using modern SEC equipment to study the elution of polymer samples of different chemical species and various molecular architectures. All samples have a narrow distribution of both molecular weight and molecular architecture. Chemically they consist of two groups: model polyethylene and polystyrene, derived by means of anionic polymerization and subsequent saturation or coupling reactions. The polyethylene samples include linear chains, 3-arm stars, 2-branch point molecules, and multibranch point combs. The polystyrene samples are commercially available linear standards. The equipment used to study these samples consists of an SEC with an online multiangle laser light scattering (MALLS) detector, a differential refractometer index (DRI) detector, and a viscometer to determine R_g, M, $[\eta]$, and elution volume.

† Present address: 7496 Old Channel Trail, Montague, MI 49437.

* To whom correspondence should be sent.

10.1021/ma030586k CCC: $27.50
Published on Web 04/29/2004

II. Experimental Section

Instrumentation and Column Information. The measurements were performed using a Waters Alliance 2000 SEC with an on-line MALLS detector and a viscometer. A flow rate of 0.54 mL/min, 335 μL injection volume, and elution solvent 1,2,4-trichlorobenzene (TCB) were used in all experiments. The various columns, DRI detector, and viscometer are contained within an oven maintained at 135 °C.

The MALLS detector is a DAWN DSP (Wyatt Technology, Inc.). The primary components are an optical flow cell, a 30 mW, 488 nm argon ion laser light source, and an array of 17 photodiodes placed at collection angles from 17.7° to 154.8°. A heated transfer line, maintained at 135 °C, conducts the stream emerging from the SEC columns out of the oven and into the optical flow cell (also maintained at 135 °C) and then back into the oven to the DRI detector. The viscometer is inherent to the Alliance 2000 and is based on a design patented by Waters Corp.[21] It consists of three capillaries, two holdup reservoirs, and two transducers. The relative viscosity $\eta_{rel}(c) = \eta(c)/\eta_{solvent}$ is determined from the pressure transducers. The viscometer is located downstream of the DRI detector.

The columns used are three Polymer Laboratories PLgel 10 μm Mixed B LS (light scattering) columns. The manufacturer stated molecular weight range for separation (for polystyrene) is 500−10 000 000 g/mol. Using these columns under the conditions described above, we typically measure an M/M_n of 1.07 for polystyrene standards with a manufacturer stated value of 1.03. The difference may be attributed to band broadening. No corrections for band broadening were done as they were deemed unnecessary for this study.

Detector Calibration. The DRI detector, which uses a 880 nm light source, was calibrated by injecting known quantities of various polyethylene standards that include National Institute of Standards and Technology standards—NIST 1482, NIST 1483, NIST 1484, NIST 1475—and ExxonMobil Exceed 1018. The integrated chromatograph areas are proportional to the product of polymer concentration and refractive index increment, the proportionality constant being the DRI response factor. In calculating response factors for polystyrene and polyethylene, we used dn/dc values determined at 488 nm, as these are not available at 880 nm. As a result, the polystyrene response factor was about 10% lower than the polyethylene response factor, a reasonable result given expectations that the dispersion in dn/dc for polyethylene will be different from that for polystyrene.[22]

The MALLS detector was calibrated by measuring the 90° scattering intensity of the elution solvent TCB at 135 °C. For these conditions, the Rayleigh ratio of TCB at 488 nm is 1.065×10^{-4} cm^{-1}.[23] We normalized the photodetectors by injecting a low molecular weight polyethylene, NIST 1482 with a certificate M_w of 13 600 g/mol,[24] which scatters light nearly isotropically. On the basis of extrapolations of our own and literature data for polyethylenes of higher molecular weight, we estimate $R_g = 5$ nm for NIST 1482, a size which corresponds to an ≈1% asymmetry in scattering intensity between the lowest and highest scattering angles.[25]

The viscometer was calibrated by injecting NIST 1482, NIST 1483, and NIST 1484, whose values of $[\eta]$ in TCB at 130 °C are certified with an expected limit of systematic error of 1%.[24] The viscometer calibration constant was then adjusted to match, on average, those stated intrinsic viscosity values.

Interdetector volumes for the SEC−MALLS−viscometer configuration were determined from shifts in elution volume of the refractive index, light scattering, and viscometer chromatographs for a narrow MWD polystyrene standard having a stated upper limit of $M_w/M_n = 1.02$.

Sample Information. The polyethylene model polymers are anionically polymerized, polybutadiene polymers that have been hydrogenated to form ethylene−butene copolymers of 8 wt % butene. They can be classified into four structure types: linear, 3-arm stars, 2-branch point, and comb structures. The details of their synthesis and characterization have been described elsewhere.[26] The molecular weights of the linear samples ranged from 6500 to 850 000 g/mol. As measured under the conditions described above, M_w/M_n ranges from 1.07 to 1.20, with the more heavily branched polymers generally having higher M_w/M_n. The linear polystyrenes were purchased from Polymer Laboratories. Their molecular weights ranged from 10 000 to 2 800 000 g/mol; nominal M_w/M_n ranged from 1.02 to 1.06.

Solution Preparation and Operating Procedures. The elution solvent was prepared by adding approximately 1.5 g of the antioxidant 2,6-di-*tert*-butyl-4-methylphenol (BHT) per liter to reagent grade TCB (Aldrich) and then filtering through a 0.7 μm glass prefilter followed by a 0.1 μm Teflon filter. Most of this solvent was used as the SEC mobile phase, with a small aliquot retained for polymer solution preparation. The solvent was passed through an on-line degasser before entering the SEC.

Polymer solutions were prepared by placing dry polymer in a glass container, adding the desired amount of TCB, covering the container with a Teflon-lined cap, and then heating the mixture at 160 °C with continuous agitation for 2 h. All quantities were measured gravimetrically. Polymer concentration was expressed in mass/volume units with a TCB density of 1.324 g/cm^3 at 135 °C. The concentrations chosen varied with sample. The considerations in determining the optimum solution concentration for a given sample were signal-to-noise, the effect of the second virial coefficient on determining molecular weight, and potential elution volume shifts due to column overloading.

III. Data Analysis

Basic Formalisms. The MALLS data, taken at 488 nm, were analyzed with the standard formulas for static light scattering[22]

$$\frac{K_0 c}{\Delta R(\theta,c)} = \frac{1}{MP(\theta)} + 2A_2 c \qquad (1)$$

Here, $\Delta R(\theta,c)$ is the excess Rayleigh scattering intensity at scattering angle θ, c is the polymer concentration, M is the polymer molecular weight, A_2 is the second virial coefficient, $P(\theta)$ is the form factor, and $K_0 = 4\pi^2 n^2 (\mathrm{d}n/\mathrm{d}c)^2/\lambda^4 N_a$ is the optical constant for the system. Here n is the refractive index of the solvent, λ the in vacuo wavelength of the incident light, N_A is Avogadro's number, and dn/dc is the refractive index increment for the system. The concentrations used in the analyses are the values measured from the DRI output.

The viscometry data were analyzed with the Huggins equation $\eta_{sp} = c[\eta] + k_H[\eta]^2 c^2$, where $[\eta]$ is the intrinsic viscosity of the polymer and k_H is the Huggins coefficient.[10] We use a good solvent value of $k_H = 0.3$ for all samples in this study.[10]

The equations above describe how M, R_g, and $[\eta]$ are extracted from the experimental data. However, the data analysis requires knowledge of the parameters $P(\theta)$, dn/dc, and A_2. We now discuss the values used in analyzing the data and their effect on the results.

Form Factor The random-coil form factor[22] was used for all linear samples:

$$P(u) = \frac{2[\exp(-u) - 1 + u]}{u^2} \qquad (2)$$

where $u = 16\pi^2 n^2 R_g^2 \sin^2(\theta/2)/\lambda^2$. Here, θ is the angle of the scattered light relative to the incident beam.

The issue now arises as to which form factors to use for analyzing samples with LCB. In principle, we should derive the form factors for the various architectures and then fit the data to eq 1 using those form factors. Unfortunately, although the form factors for the simpler structures are known, those for the more complex

Table 1. Comparison of NIST Certificate M_w Values and Measured Values (Averaged over 5 Runs) Using dn/dc = −0.109

NIST standard	certificate M_w (g/mol)	measured M_w (g/mol)
NIST 1482	13 600	12 600
NIST 1483	32 100	32 900
NIST 1484	119 600	121 200

structures are not. The suggested method for analyzing data in this situation is to fit the data to a higher-order polynomial form and then extrapolate to the small angles to determine R_g. However, this has an obvious disadvantage in that increasing the number of fitting parameters reduces their reliability. Instead, we choose to apply eq 2, regardless of whether they contain LCB or not. A general sense of the error in doing this can be obtained by comparing to the form factors of a symmetric 3-arm star[22]

$$P(u) = \frac{14}{9u} + \frac{98}{27u^2}[\exp(-6u/7) - \exp(-3u/7)] \quad (3)$$

and a hard sphere, the limiting case of a hyperbranched structure:[22]

$$P(u) = \frac{81}{125u}[\sin\sqrt{5u/3} - \sqrt{5u/3}\cos\sqrt{5u/3}]^2 \quad (4)$$

The values of R_g for the samples with LCB range from 14 to 28 nm. We generated artificial sets of light scattering data for $R_g = 20$ and 30 nm symmetric 3-arm stars (eq 3) and hard spheres (eq 4). We then fit these artificial data sets to a random-coil form factor (eq 2). For the symmetric 3-arm stars we obtain R_g values which are 0.5% and 1.0% high, differences which are within the measurement error. For the hard spheres we obtain R_g values which are 2.5% and 5.6% high. These differences are higher than the measurement error. However, it should be kept in mind that by choosing to compare to a hard sphere form factor, we are determining the upper limit of error. None of the samples studied here are so highly branched to be considered as resembling hard spheres; therefore, the error introduced by assuming a random-coil form factor would be lower.

Refractive Index Increment. Pope and Chu reported dn/dc = −0.109 cm^3/g at λ = 488 nm for polyethylene in TCB at 135 °C.[27] We used this value (with small corrections for M_n dependence to be discussed later) to analyze the NIST standards that were run periodically during this study. Table 1 compares the M_w results we obtained (average over five runs) to the NIST certified values. The values we obtained are close to the NIST certificate values. If the Pope−Chu value was significantly wrong, we would expect to see a larger discrepancy since the M_w value obtained is inversely proportional to (dn/dc)^2. Therefore, we accept and use the dn/dc value of −0.109 for polyethylene. However, strictly speaking the polyethylene model polymers are not polyethylene but are ethylene−butene copolymers with 8 wt % butene. In a previous study we found that dn/dc for EB copolymers exhibits a weak dependence on butene content, $(dn/dc)_{EB} = (dn/dc)_{PE}(1 - 0.126w)$, where w is the weight fraction of butene.[25] We therefore used a dn/dc value of −0.108 for the polyethylene model polymers.

To our knowledge, no measurements of dn/dc have been made for polystyrene in TCB at 135 °C. Nor could we adequately measure it from the DRI response because the DRI uses an 880 nm wavelength, not the 488 nm wavelength used by the MALLS. In view of this, we simply accepted the manufacturer stated values of M for the standards and adjusted dn/dc so as to obtain on average the same values. We found a dn/dc value of 0.047 would do this. As an independent check, we verified the molecular weight of the nominal 135 000 g/mol standard in two ways. First, we used a Brookhaven 2030 goniometer setup[28] to perform a Zimm analysis with tetrahydrofuran as the solvent and a 632.8 nm laser as the light source (a well-known system). Second, we had the sample analyzed by matrix-assisted laser desorption ionization (MALDI). The two analyses gave M_w values of 137 300 and 131 400 g/mol respectively, both close to the stated value.

The final issue with respect to dn/dc is its variation with molecular weight. Because of chain ends effects, dn/dc varies almost linearly with $1/M_n$, reaching asymptotic limits at high molecular weights.[19] To account for this effect, we measured the DRI chromatograph areas for a series of low molecular weight polyethylene and polystyrene samples. (A Waters Corp. 150C SEC was used because its DRI white light source is a closer approximation to the 488 nm laser wavelength than the 880 nm source of the Waters Corp. Alliance 2000 SEC.) The polyethylene samples used are a combination of commercial samples from NIST, Polymer Laboratories, and Petrolite Corp. The M_n range for this set of five samples is from 500 to 27 000 g/mol. The anionically polymerized polyethylene samples were not used because they did not extend to sufficiently low molecular weights. The polystyrene samples used were five molecular weight standards from Polymer Laboratories with $575 \le M_n \le 30\,000$ g/mol. Accepting asymptotic limits of −0.109 and 0.047 for polyethylene and polystyrene, respectively, we determine a functional form of $(dn/dc)_{PE} = -0.109(1 + 176/M_n)$ for polyethylene and $(dn/dc)_{PS} = 0.047(1 - 391/M_n)$ for polystyrene. The correlation coefficients are $R = 0.993$ and 0.998, respectively. We use these functional forms to calculate the appropriate dn/dc, with a −0.108 prefactor in place of the −0.109 for the model polyethylene samples. The polyethylene M_n dependence can easily be shown to be very reasonable on the basis of refractive index and density data for n-alkanes and the approach to dn/dc calculations described in ref 19. Similarly, the M_n dependence for polystyrene is quite consistent with results from ref 19.

Second Virial Coefficient. In dilute solution scattering A_2 is a second-order term whose relative importance is determined by the quantity $2A_2Mc$. In this study efforts were made to ensure that $2A_2Mc$ is much less than unity. Nevertheless, for the sake of completeness it is desirable to properly account for A_2 in analyzing the data. To do this, we use a previously determined correlation between A_2 and R_g for polyolefins in TCB, $A_2 = 1.07 \times 4\pi R_g^3 N_A/3M_w^2$.[25]

Hence, by measuring R_g and M_w, we can estimate an appropriate A_2. The data are then reanalyzed with eq 1 using the A_2 value thus obtained. This procedure is applied to all samples.

Region of Integration. Some of the branched polyethylenes analyzed contained remnants of unreacted material (see ref 26 for explanations and figures).[26] Hence, to ensure that the signals we analyze are from the intended polymer structure, we integrated only over

Table 2. Tabulation of Results for the Linear Model Polymers[a]

sample designation	target structure (g/mol)	mol wt (g/mol)	R_g (nm)	$[\eta]$ (dL/g)	elution vol (mL)	predicted g	measured g	measured g'
PEL193	195 000	182 700	25.1	2.510	19.714	1.00	1.01	0.99
PEL125	127 000	119 900	19.6	1.849	20.198	1.00	1.01	0.98
PEL147	148 000	139 000	21.4	2.088	20.023	1.00	1.01	1.00
PEL90	90 200	84 800	15.9	1.451	20.559	1.00	0.99	0.99
PEL243	255 000	249 800	29.8	3.163	19.323	1.00	0.99	1.00
PEL280	290 000	279 100	32.0	3.430	19.191	1.00	1.00	1.01
PEL685	789 000	832 900	60.7	7.658	17.856	1.00	1.00	1.04
PEL98	98 000	97 500	17.1	1.595	20.425	1.00	0.98	0.98
PEL19	19 300	18 400	6.5*	0.530	22.084	1.00		1.06
PEL42	42 000	39 100	10.1*	0.845	21.356	1.00		0.99
PEL40	40 000	44 100	10.9*	0.918	21.241	1.00		0.99
PEL53	53 000	49 700	11.7*	1.003	21.110	1.00		0.99
PEL6.5	6 500	6 600	3.6*	0.237	23.213	1.00		0.97

[a] The radii of gyration for the five lowest molecular weight samples were obtained from extrapolation of the R_g vs MW plot shown in Figure 2a.

Table 3. Tabulation of Results for the 3-Arm Star Polymers[a]

sample designation	arm 1/arm 2/arm 3	mol wt (g/mol)	R_g (nm)	$[\eta]$ (dL/g)	elution vol (mL)	predicted g	measured g	measured g'
$PES(50)_2(5)$	52/52/5.2	127 700	19.3	1.818	20.159	0.94	0.91	0.93
$PES(50)_2(15)$	52/52/15.5	134 100	19.2	1.787	20.129	0.85	0.85	0.88
$PES(50)_2(25)$	52/52/26	126 400	18.0	1.626	20.219	0.81	0.80	0.83
$PES(19)_2(83)$	86.3/19.7/19.7	113 200	18.4	1.702	20.304	0.90	0.95	0.94
$PES(43)_3$	44.5/44.5/44.5	130 600	17.7	1.630	20.176	0.78	0.75	0.82
$PES(50)_3$	65/65/65	184 800	22.0	2.112	19.785	0.78	0.77	0.83
$PES(15)_2(85)$	88.5/15.5/15.5	122 800	18.5	1.754	20.214	0.93	0.87	0.92
$PES(48)_3$	50/50/50	127 700	17.2	1.669	20.173	0.78	0.72	0.85
$PES(49)_2(5)$	65/50/5.5	103 200	17.1	1.535	20.414	0.94	0.92	0.91
$PES(49)_3$	48/48/48	147 700	20.0	1.874	20.033	0.78	0.82	0.86
$PES(28)_3$	28/28/28	83 300	13.8	1.226	20.631	0.78	0.77	0.84
$PES(55)_3$	55/55/55	146 700	19.3	1.859	20.004	0.78	0.77	0.86
$PES(47)_3$	47/47/47	126 100	17.8	1.667	20.179	0.78	0.78	0.86

[a] Arm 1, arm 2, and arm 3 refer to the target arm lengths in kg/mol.

Table 4. Tabulation of Results for the 2-Branch Point Structures[a]

sample designation	connector/arm/ no. of arms	mol wt (g/mol)	R_g (nm)	$[\eta]$ (dL/g)	elution vol (mL)	predicted g	measured g	measured g'
$PEH(10)_2(95)(10)_2$	99.4/10.3/2	162 200	22.9	2.132	19.890	0.95	0.97	0.92
$PESH(10)_3(107)(10)_3$	111/10.5/3	186 500	23.0	2.236	19.767	0.89	0.83	0.87
$PEPP(10)_5(92)(10)_5$	95.4/10.8/5	229 400	25.6	2.196	19.681	0.73	0.81	0.74
$PEH(50)_2(25)(50)_2$	25/51.5/2	198 800	20.1	1.906	19.772	0.67	0.59	0.71
$PEH(18)_2(130)(18)_2$	93.8/18.1/2	172 000	22.7	2.095	19.927	0.89	0.89	0.87
$PESH(18)_3(130)(18)_3$	93.8/18.1/3	194 000	23.4	2.144	19.811	0.78	0.82	0.81
$PEPP(15)_5(125)(15)_5$	95.8/14.6/5	274 000	25.5	2.142	19.585	0.67	0.65	0.64
$PEPP(20)_5(134)(20)_5$	95/19.5/5	308 800	26.3	2.207	19.396	0.60	0.60	0.60
$PEPP(20)_5(111)(20)_5$	72/19.7/5	264 000	25.8	2.160	19.564	0.54	0.69	0.66
$PEH(25)_2(76)(25)_2$	25.8/24.9/2	90 100	13.9	1.264	20.531	0.71	0.71	0.82
$PEH(22)_2(145)(22)_2$	101/22/2	181 900	24.9	2.460	19.786	0.88	1.00	0.98
$PESH(22)_3(140)(22)_3$	96/22/3	241 700	26.7	2.397	19.604	0.75	0.82	0.78
$PEPP(12)_5(104)(12)_5$	80/12/5	179 700	22.0	1.825	19.953	0.67	0.79	0.73

[a] "Connector" and "arm" refer to the target connector and arm lengths in kg/mol (refer to Figure 1).

the central peak region, defined as the elution volume region ±0.25 to ±0.30 mL from the peak maximum. For consistency, this was done for all samples: linear polyethylene, branched polyethylene, and linear polystyrene.

IV. Experimental Results

Tabulation of Measurement Results. Tables 2−6 contain the experimental results for the model polyethylene and polystyrene standards. The molecular weights, R_g, and $[\eta]$ are weight-averaged values obtained by integrating over the central peak region. The elution volumes are values measured at the DRI peak maximum. R_g values with an asterisk (*) alongside are values extrapolated from the scaling laws derived from the higher molecular weight samples (see Figure 2a). For the linear polyethylene samples

$$R_g = 2.085 \times 10^{-2} M^{0.585}$$
$$[\eta] = 4.934 \times 10^{-4} M^{0.705} \quad (5)$$

and for linear polystyrene

$$R_g = 8.68 \times 10^{-3} M^{0.615}$$
$$[\eta] = 1.311 \times 10^{-4} M^{0.700} \quad (6)$$

These formulas are consistent with those found for other good solvent systems.[29]

The last two columns are the measured Zimm−Stockmayer (Z−S) branching indices defined as $g =$

Table 5. Tabulation of Results for the Comb Model Polymers[a]

sample designation	backbone/arm/ no. of arms	mol wt (g/mol)	R_g (nm)	$[\eta]$ (dL/g)	elution vol (mL)	predicted g	measured g	measured g'
PEC(101)-g-$(7)_{30}$	105/6.7/34	368 100	25.6	1.819	19.429	0.35	0.46	0.44
PEC(97)-g-$(23)_{26}$	101/24.4/21.9	590 200	28.3	2.104	18.947	0.25	0.33	0.36
PEC(100)-g-$(5)_2$	104/5.4/2.1	108 000	17.9	1.665	20.334	0.91	0.95	0.95
PEC(100)-g-$(5)_{12}$	104/5.4/14.8	165 200	19.5	1.649	20.045	0.60	0.69	0.70
PEC(108)-g-$(6)_{12}$	112/4.9/12	160 800	19.7	1.736	20.034	0.68	0.72	0.75
PEC(92)-g-$(10)_1$	108/11.3/0.7	105 100	16.9	1.522	20.395	0.94	0.88	0.89
PEC(101)-g-$(5)_{12}$	105/5.7/11	219 600	21.5	1.713	19.827	0.66	0.60	0.60
PEC(92)-g-$(10)_5$	108/11.3/10.7	128 300	17.3	1.566	20.228	0.54	0.73	0.79
PEC(57)-g-$(22)_{15}$	56.5/22/15	510 000	23.8	1.713	19.192	0.28	0.27	0.33
PEC(96)-g-$(10)_{17}$	96/5/16.2	214 200	21.0	1.689	19.817	0.57	0.59	0.60
PEC(96)-g-$(12)_{16}$	96/12/15.6	267 700	22.9	1.782	19.650	0.41	0.54	0.54

[a] "Backbone" and "arm" refer to the target backbone and arm lengths in kg/mol. "Number of arms" is the average number of arms placed randomly along the backbone.

Table 6. Tabulation of Results for the Polystyrene Standards[a]

sample designation	nominal mol wt (g/mol)	mol wt (g/mol)	R_g (nm)	$[\eta]$ (dL/g)	elution vol (mL)	predicted g	measured g	measured g'
PS 2.88 M	2 880 000	2 569 000	76.5	4.195	17.500	1.00	1.01	1.04
PS 1.73 M	1 730 000	1 733 000	59.5	3.181	18.009	1.00	1.00	1.04
PS 1.0 M	1 000 000	949 400	41.2	2.028	18.714	1.00	1.00	1.01
PS 667.5 K	667 500	659 900	32.9	1.536	19.184	1.00	1.00	0.99
PS 629.5 K	629 500	624 300	31.9	1.491	19.251	1.00	1.00	1.00
PS 483 K	483 000	449 500	25.8	1.201	19.645	1.00	0.98	1.01
PS 390 K	390 000	395 700	23.6	1.079	19.809	1.00	0.96	0.99
PS 283 K	283 000	277 800	19.6	0.834	20.262	1.00	1.03	0.98
PS 220.5 K	220 500	223 900	17.1	0.721	20.506	1.00	1.01	0.99
PS 135 K	135 000	135 600	12.4*	0.498	21.051	1.00		0.97
PS 65.5 K	65 500	66 500	8.0*	0.299	21.796	1.00		0.96
PS 30.3 K	30 300	29 100	4.8*	0.171	22.695	1.00		0.98
PS 10.05 K	10 050	9800	2.5*	0.084	23.947	1.00		1.03

[a] The radii of gyration for the four lowest molecular weight samples are values obtained from extrapolation of the polystyrene R_g vs MW plot shown in Figure 2a.

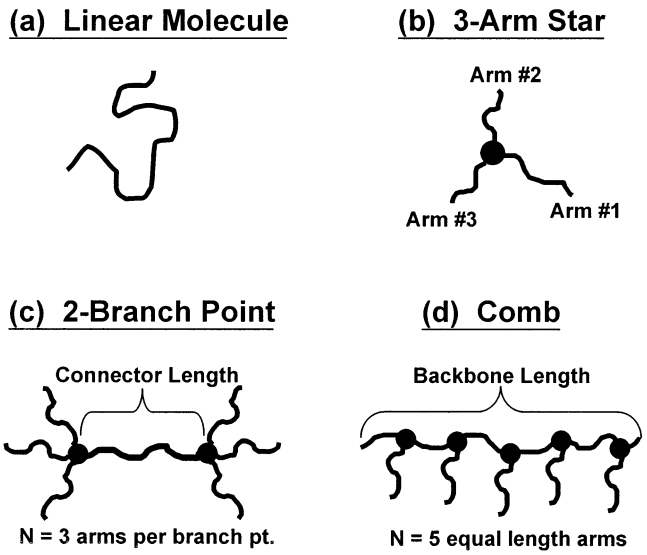

Figure 1. Four categories of model polymers. (a) Linear molecules, (b) 3-arm stars. Arm lengths are defined as the distance from the branch point to the end of the arm, (c) 2-branch point structures. The connector is defined as the length between the branch points. Excluding connector, each branch points has n equal length arms, and (d) combs. The combs have n equal length arms placed randomly along the backbone.

$\langle R_g^2\rangle_{LCB}/\langle R_g^2\rangle_{linear}$ and $g' = [\eta]_{LCB}/[\eta]_{linear}$.[30] Here, $\langle R_g^2\rangle_{LCB}$ and $[\eta]_{LCB}$ refer to the values for the given structures, and $\langle R_g^2\rangle_{linear}$ and $[\eta]_{linear}$ refer to the values for a linear molecule with the same total molecular weight. Values of $\langle R_g^2\rangle_{linear}$ and $[\eta]_{linear}$ were obtained by applying the expressions in eq 5 using the measured M. For a 3-arm star the predicted Z−S branch index for random walk molecules is given by[30]

$$g = \sum_{v=1}^{3}\left[\frac{3N_v^2}{N^2} - \frac{2N_v^3}{N^3}\right] \tag{7}$$

where N_v refers to the molecular weight of arm v and N refers to the total molecular weight. For the 2-branch point structures the predicted Z−S branch index is[30]

$$g = 6\left[2n\left(\frac{N_{arm}^2}{2N^2} - \frac{N_{arm}^3}{3N^3}\right) + \left(\frac{N_{con}^2}{2N^2} - \frac{N_{con}^3}{3N^3}\right) + \frac{N_{con}(nN_{arm})^2}{N^3}\right] \tag{8}$$

where n is the number of equal length arms (excluding connector) connected to each branch point, N_{arm} is the molecular weight of the arm, N_{con} is the molecular weight of the connector between the branch points, and N is the total molecular weight (see Figure 1c for definition of terms). Finally, for random walk comb structures the Z−S branch index is[31,32]

$$g = \frac{N_{bb}^3}{N^3} + \frac{2nN_{bb}^2N_{arm}}{N^3} + \frac{n(n+2)N_{arm}^2N_{bb}}{N^3} + \frac{(3n^2-2n)N_{arm}^3}{N^3} \tag{9}$$

where N_{bb} is the backbone molecular weight, n is the average number of equal molecular weight arms con-

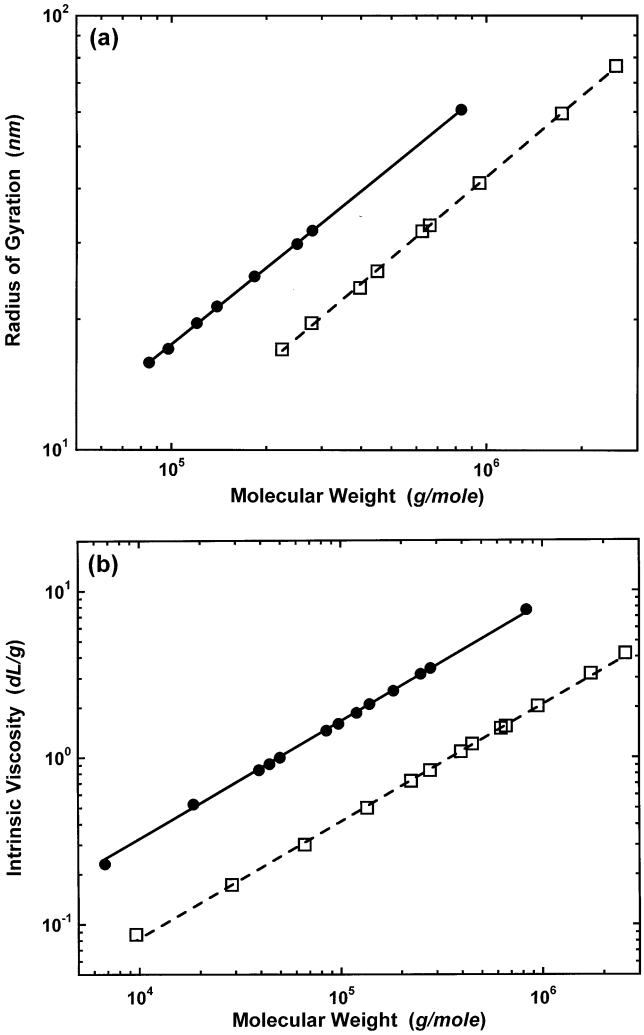

Figure 2. Log−log plots of (a) R_g vs MW and (b) [η] vs MW for the linear model polyethylene (●) and polystyrene (□) samples in TCB at 135 °C. The R_g scaling laws are used to extrapolate values for lower molecular weight samples. The solid and dashed lines are fits to the polyethylene and polystyrene data, respectively.

nected to the backbone, and N_{arm} is the molecular weight of the arms.

Comparison with Theory and Past Experimental Results. Before addressing the nature of SEC separation, it is useful to compare the experimental results for the LCB model polymers to theory and previous experimental results. In Figure 3, we plot our measured values of g with those predicted for random walk molecules according to eqs 7−9. A reasonably good match between prediction and experiment is evidently obtained. For the case of symmetric 3-arm stars we fit the R_g and [η] data using the linear chain exponents, 0.585 and 0.705, respectively, and obtain prefactors of 1.829×10^{-2} nm and 4.167×10^{-4} dL/g, with correlation coefficients of $R = 0.989$ and 0.992. The former corresponds to a branch index of $g = 0.77$, which is close to the 0.78 value predicted for symmetric 3-arm stars with eq 7 and experimentally observed by Roovers in different good-solvent systems.[33] The latter gives $g' = 0.84$, which is close to the $g' = 0.82-0.83$ values experimentally observed in other good-solvent systems.[33]

Experimental results on 2-branch point molecules are sparse. To our knowledge, the only detailed dilute solution work were obtained by Roovers and Toporowski

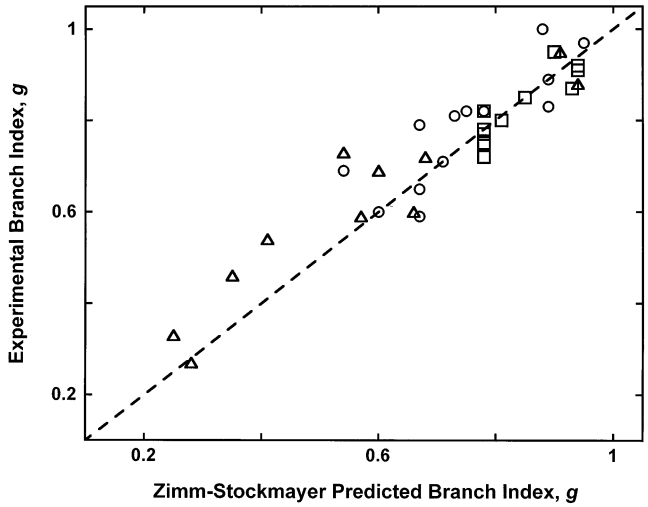

Figure 3. Measured vs Zimm−Stockmayer predicted branch indices for 3-arm stars (□), 2-branch point molecules (○), and combs (△).

on regular H-polymers (five equal length strands joined to form a molecule with two trifunctional branch points).[34] In a good-solvent system they measured $g = 0.69$ and $g' = 0.80$; from eq 8, the value of g for regular-H random walks is 0.712, in fair agreement with the good-solvent data. The closest approximation to a regular H-polymer in our sample set is PEH$(25)_2(76)(25)_2$, for which $g = 0.71$ and $g' = 0.82$, both reasonably close to the Roovers and Toporowski values.

Contrary to the case of 2-branch point database, there exists a substantial body of past work done on dilute solution properties of comb polymers in both good and Θ solvent conditions.[35,36] Figure 4a compares past and present dilute solution results on comb polymers. We note two features. First, the experimental g values are, for the most part, larger than the predicted values even under Θ-solvent conditions. Roovers suggested that this is due to the increased likelihood of triple contacts in more densely branched polymers. Second, as shown in Figure 4b, g and g' for combs seemingly follow a $g' = g^{\epsilon}$ relationship with $\epsilon = 0.85$. The theoretical ϵ value for symmetric stars is 0.50.[37] There is no prediction of a $g' = g^{\epsilon}$ relationship for combs, nor any expectation that there should be one.

Universal SEC Calibration. We now come to the main question: Upon what general size basis, if there is one, does SEC separate molecules? We examine two situations: linear molecules of different chemical species and molecules with different types of LCB.

For the species dependence, consider the plots of R_g^3 and [η]M vs elution volume in parts a and b of Figure 5 respectively for the linear polyethylene and polystyrene samples. The linear polyethylene and polystyrene samples follow a common R_g^3 curve over essentially the entire range of sizes (Figure 5a). They also follow a common [η]M curve in the large size range, but they clearly begin to diverge as the size decreases, forming separate curves with linear polyethylene eluting before linear polystyrene at equal values of [η]M. This species-dependent deviation at low molecular weights, also with polyethylene eluting before their polystyrene counterparts, has been observed in another solvent.[19] At this point it is necessary to consider the possibility that the perceived deviation from [η]M universality may arise from some systematic error in the data analysis, perhaps through an incorrect accounting of dn/dc as the

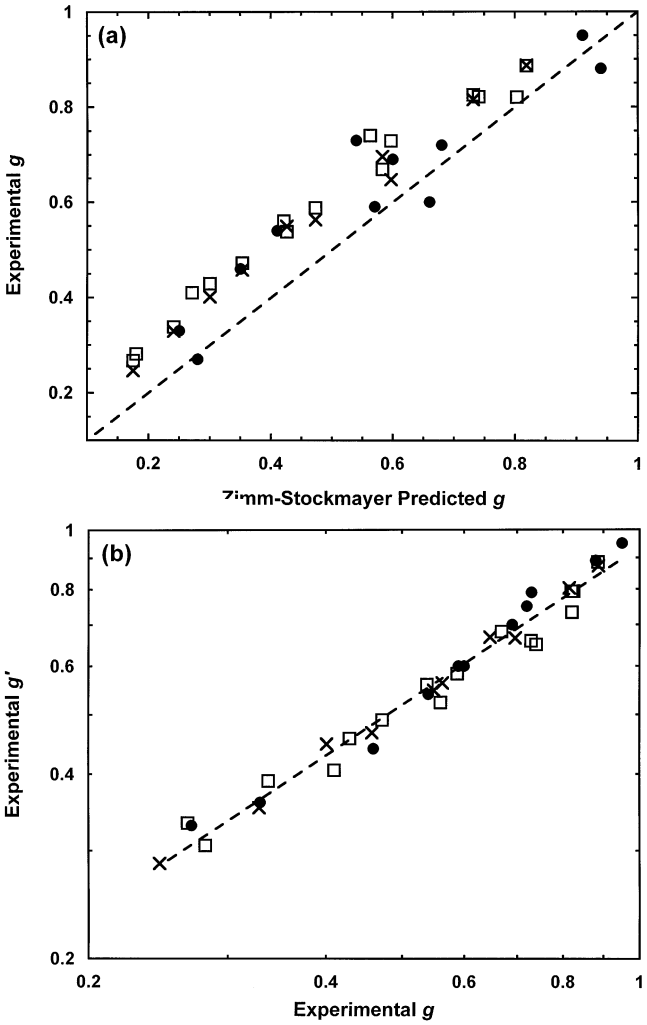

Figure 4. (a) Plot of experimental vs predicted g for comb polymers. The dashed line represents a perfect match between experiment and prediction. (b) A log−log plot of measured g' vs measured g for comb polymers. The dashed line is $g' = g^{\epsilon}$ with $\epsilon = 0.85$. The three sets of data are polyethylene in TCB at 135 °C (●), polystyrene in Θ-solvent (□),[35,36] and polystyrene in toluene (×).[35,36]

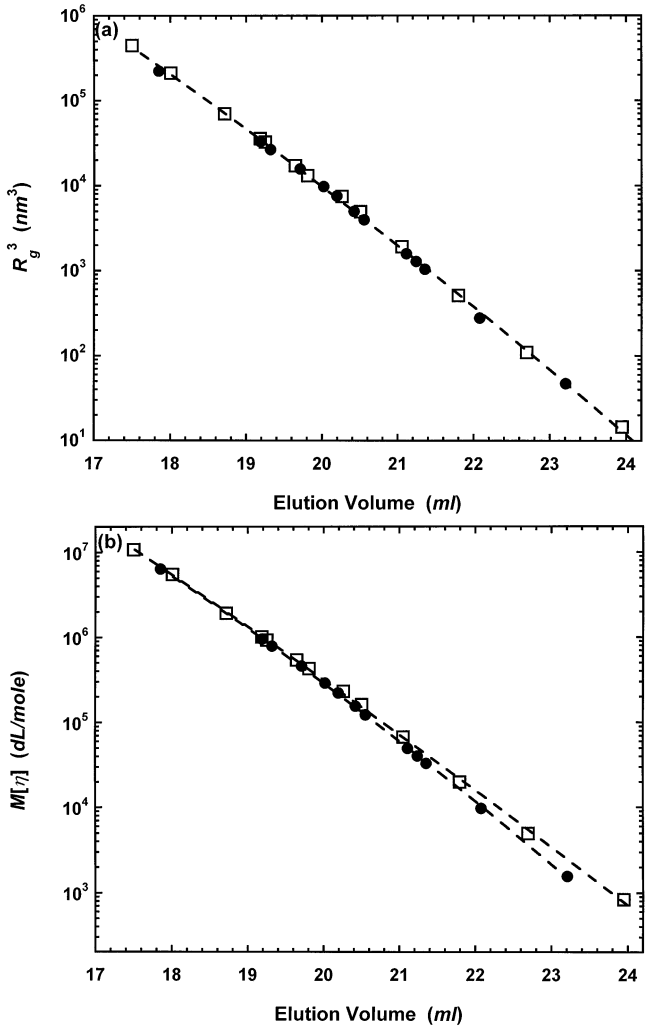

Figure 5. Semilog plots of (a) R_g^3 vs elution volume and (b) $M[\eta]$ vs elution volume for the linear model polyethylene and polystyrene samples. The linear polyethylene (●) and polystyrene (□) samples follow a single R_g^3 curve, but seemingly separate $M[\eta]$ curves.

molecular weight changes. Previously, we noted the difficulties in obtaining reliable dn/dc values. Unlike R_g determinations, which depend only weakly on dn/dc through the second-order A_2 term, molecular weight determinations depend strongly on dn/dc. Use of an incorrect dn/dc would lead to an incorrect molecular weight and thereby an incorrect value of $[\eta]M$. However, we do not feel that this can fully account for the observed deviation. The deviation at $[\eta]M = 1600$ dL/mol (the lowest molecular weight polyethylene sample) would require a combined 25% error in the dn/dc values for polystyrene and polyethylene. Such an error is significantly larger than the uncertainties in dn/dc implied by comparisons of M_w values obtained on polystyrene and polyethylene standards, as seen in Tables 1 and 6.

For the effect of long chain branching on elution volume, consider Figure 6a,b for the polyethylene samples, both linear and branched. Contrary to the case of linear molecules of different chemical species, $[\eta]M$ is a much better predictor of elution volume than R_g when LCB is present. The branched polymers deviate from the R_g^3 curve determined by linear molecules (Figure 6a), with the most heavily branched samples deviating most strongly (Figure 7a). In contrast, deviations from the $[\eta]M$ curve determined by linear polymers are weak (Figures 6b and 7b).

V. Discussion of Results and Conclusions

We are left with the puzzling result seen on Figures 6 and 7 that elution volume correlates better with V_H than with R_g for molecules with LCB. These results are disconcerting since it is generally believed that SEC is controlled by thermodynamic rather than hydrodynamic considerations. However, the physically appealing notion that SEC is a thermodynamic process determined solely by a molecule's R_g is clearly incorrect. One possible refinement may lie in considering the molecular shape, not just an average dimension such as R_g. A possible choice is the span dimension, which is the smallest volume that completely encloses the chain.[38,39] Such calculations show that linear polymer coils are not spherical in overall shape, but rather ellipsoidal.[38] One might imagine then that the ability of a molecule to enter a pore depends on the way that it is oriented with respect to the pore opening; the cross section of the chain perpendicular to the opening may be the correct measure and not the average dimension. Some recent work by Wei[40,41] indicate that branched polymers are more

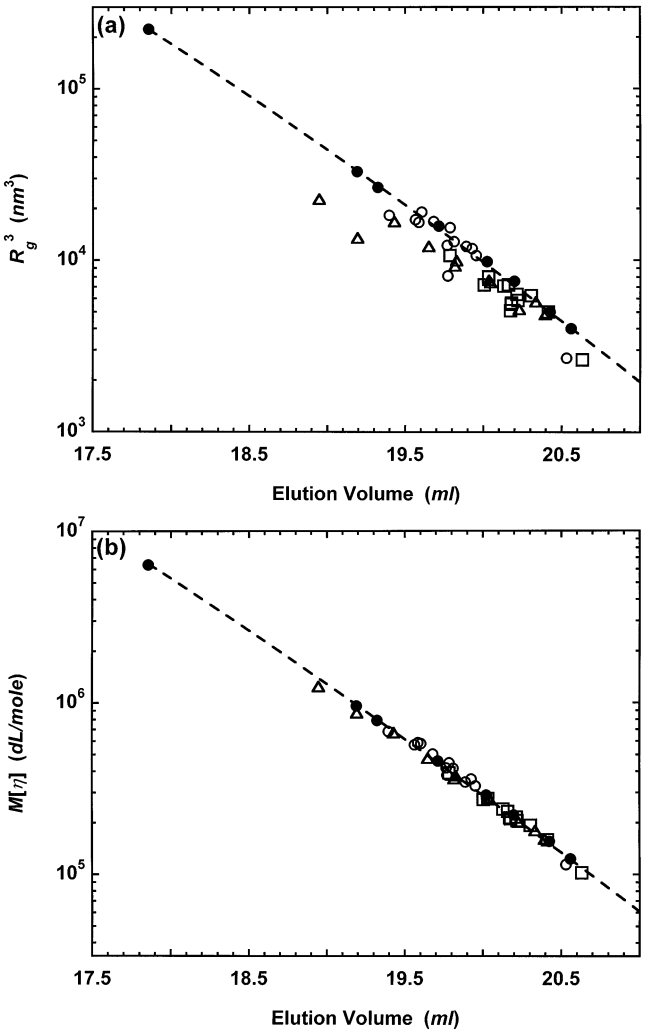

Figure 6. Semilog plots of (a) R_g^3 vs elution volume and (b) $M[\eta]$ vs elution volume for the linear and branched model polyethylene samples. The dashed lines are fits to R_g^3 and $M[\eta]$ curves for the linear molecules. The symbols represent linear molecules (●), 3-arm stars (□), 2-branch point molecules (○), and combs (△).

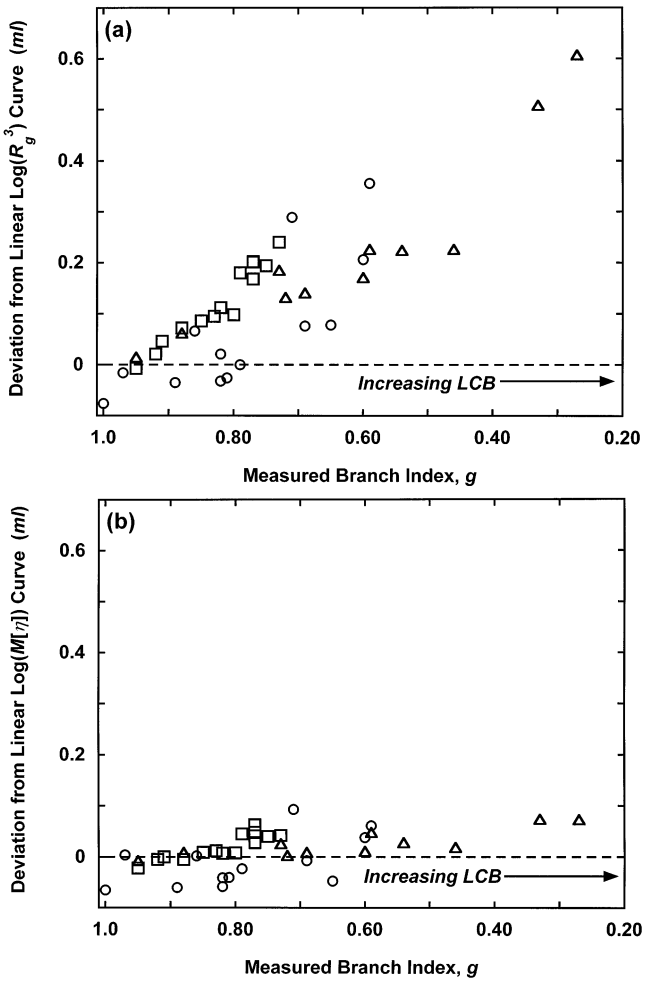

Figure 7. (a) Deviation of molecules with LCB from the R_g^3 elution curve determined by the linear molecules. (b) Deviation of molecules with LCB from the $M[\eta]$ elution curve determined by the linear molecules. The symbols represent 3-arm stars (□), 2-branch point (○), and comb (△) molecules.

symmetric than linear ones in terms of their overall shape. This may explain some of the differences between linear and branched polymers with respect to size exclusion. Similar arguments have been used to explain the failure of R_g to provide an appropriate size measure for SEC of oligomers of polyethylene and polystyrene.[19,20]

The discussion above is clearly speculative; however, a rigorous theoretical analysis has been done in the special case of symmetric stars by Casassa et al.[12,13] In their work they assumed equilibrium conditions and calculated the molecular partitioning K_f as a function of $(Nb^2/6a^2)^{1/2}$ for symmetric stars of functionality $f = 1-12$ in the cases of slab, cylindrical, and spherical pores. Here, N is the total number of chain segments in the molecule, b is the statistical segment length, a is the pore dimension, and f is the number of arms emanating from a single branch point. They observed that the theoretical predictions for all values of f for a given pore geometry superimpose onto a single line when they plot K_f as a function of $(Nb^2/6a^2)^{1/2}g^{1/6}$, which is equivalent to $(R_g/a)g^{-1/3}$. To test this prediction, we plotted (R_g^3/g) vs elution volume for all the polyethylene molecules. As predicted by Casassa et al., the symmetric 3-arm stars and linear molecules lie on a common curve. The 2-branch point and comb molecules do not lie on this curve.

The success of Casassa et al. in predicting the elution of symmetric stars indicates that similar equilibrium calculations for the other branched architectures may explain their elution behavior. Unfortunately, we know of no such work on the configurations of other branched polymers in pores. Direct calculations for complicated molecular structures are likely to be extremely challenging, although simulations may be possible. We encourage those with such skills to apply them to the problem of SEC.

Acknowledgment. We gratefully acknowledge J. Ball, B. Chapman, P. Eiselt, D. Higgins, C. Pavlick, M. Thomas, Y. Wade, and D. Winesett for their assistance in doing this work. We also acknowledge L. Fetters, N. Hadjichristidis, and P. Wright for synthesizing the model polyethylene samples.

References and Notes

(1) Mandelkern, L. In *Physical Properties of Polymers*, 2nd ed.; Mark, J. E., et al., Eds.; American Chemical Society: Washington, DC, 1993; Chapter 4.
(2) Ward, I. M. *Mechanical Properties of Solid Polymers*, 2nd ed.; J. Wiley & Sons: New York, 1983.

(3) Peacock, A. J. *Handbook of Polyethylene*; Marcel Dekker: New York, 2000.
(4) Graessley, W. W. In *Physical Properties of Polymers*, 2nd ed.; Mark, J. E., et al., Eds.; American Chemical Society: Washington, DC, 1993; Chapter 3.
(5) Moore, J. C. *J. Polym. Sci., Part A* **1964**, *2*, 835.
(6) Yau, W. W.; Kirkland, J. J.; Bly, D. D. *Modern Size Exclusion Liquid Chromatography*; John Wiley & Sons: New York, 1979.
(7) Wu, C.-S., Ed. *Handbook of Size Exclusion Chromatography*; Dekker: New York, 1995.
(8) Glockner, G. *Polymer Characterization by Liquid Chromatography*; Elsevier Science: New York, 1987.
(9) Grubisic, Z.; Rempp, P.; Benoit, H. *J. Polym. Sci., Polym. Lett.* **1967**, *5*, 753.
(10) Yamakawa, H. *Modern Theory of Polymer Solutions*; Harper & Row: New York, 1971.
(11) Casassa, E. F. *J. Polym. Sci., Polym. Lett.* **1967**, *5*, 773.
(12) Casassa, E. F.; Tagami, Y. *Macromolecules* **1969**, *2*, 14.
(13) Casassa, E. F. *Sep. Sci.* **1971**, *6*, 305.
(14) Giddings, J. C.; Kucera, E.; Russell, C. P.; Meyers, M. N. *J. Phys. Chem.* **1968**, *72*, 14.
(15) De Gennes, P.-G. *Scaling Concepts in Polymer Physics*; Cornell University Press: Ithaca, NY, 1979.
(16) Davidson, M. G.; Suter, U. W.; Deen, W. M. *Macromolecules* **1987**, *20*, 1141.
(17) Roovers, J. *Polymer* **1979**, *20*, 843.
(18) Stogiou, M.; Kapetanaki, C.; Iatrou, H. *Int. J. Polym. Anal. Charact.* **2002**, *7*, 273.
(19) Chance, R. R.; Baniukiewicz, S. P.; Mintz, D.; Ver Strate, G.; Hadjichristidis, N. *Int. J. Polym. Anal. Charact.* **1995**, *1*, 3.
(20) Boyd, R. H.; Chance, R. R.; Ver Strate, G. *Macromolecules* **1996**, *29*, 1182.
(21) De Corral, J. L. United States Patent #5,637,790.
(22) Huglin, M. B. *Light Scattering from Polymer Solutions*; Academic Press: New York, 1972.
(23) Value obtained from Wyatt Technology Corp.
(24) National Institute of Technology & Standards Certification Sheets for NIST 1482, NIST 1483, and NIST 1484.
(25) Sun, T.; Brant, P.; Chance, R. R.; Graessley, W. W. *Macromolecules* **2001**, *34*, 6812.
(26) Hadjichristidis, N.; Xenidou, M.; Iatrou, H.; Pitsikalis, M.; Poulos, Y.; Avgeropoulos, A.; Sioula, S.; Paraskeva, S.; Velis, G.; Lohse, D. J.; Schulz, D. N.; Fetters, L. J.; Wright, P. J.; Mendelson, R. A.; Garcia-Franco, C. A.; Sun, T.; Ruff, C. J. *Macromolecules* **2000**, *33*, 2424.
(27) Pope, J. W.; Chu, B. *Macromolecules* **1984**, *17*, 2633.
(28) Sun, T.; King, H. E. *Macromolecules* **1996**, *29*, 3175.
(29) Fetters, L. J.; Hadjichristidis, N.; Lindner, J. S.; Mays, J. W. *J. Phys. Chem. Ref. Data* **1994**, *23*, 619.
(30) Zimm, B. H.; Stockmayer, W. H. *J. Chem. Phys.* **1949**, *17*, 1301.
(31) Berry, G. C. *J. Polym. Sci., Part A2* **1968**, *6*, 1551.
(32) Derivation by S. T. Milner at ExxonMobil Corporate Strategic Research Laboratories.
(33) Roovers, J. In *Star and Hyperbranched Polymers*; Mishra, M. K., Kobayashi, S., Eds.; Marcel Dekker: New York, 1999; Chapter 11.
(34) Roovers, J.; Toporowski, P. M. *Macromolecules* **1981**, *14*, 1174.
(35) Roovers, J. E. L. *Polymer* **1975**, *16*, 827.
(36) Roovers, J. *Polymer* **1979**, *20*, 843.
(37) Zimm, B.; Kilb, R. W. *J. Polym. Sci.* **1959**, *37*, 19.
(38) Rubin, R. J. *J. Chem. Phys.* **1972**, *56*, 5747.
(39) Hollingsworth, C. A. *J. Chem. Phys.* **1942**, *16*, 544.
(40) Wei, G. *Macromolecules* **1997**, *30*, 2125.
(41) Wei, G. *Macromolecules* **1997**, *30*, 2130.

MA030586K